Innovative models for the analysis of abrasive wheel wear in railway vehicles

J. Auciello[1], M. Ignesti[1], L.Marini[1], E. Meli[1] and A. Rindi[1]
[1]*Department of Energy Engineering, University of Florence, Italy*
E-mail: auciello@mapp1.de.unifi.it, ignesti@mapp1.de.unifi.it, marini@mapp1.de.unifi.it, meli@mapp1.de.unifi.it, rindi@mapp1.de.unifi.it

Keywords: multibody modeling, railway vehicles, wheel-rail contact, wear.

SUMMARY. In railway applications, the estimation of the wear in the wheel-rail contact is an important field of study, mainly correlated to the planning of maintenance interventions, vehicle stability and the possibility to carry out specific strategies for the wheel profile optimization. In this work Authors present a model conceived for the evaluation of the wheel profile evolution due to wear, which is organized in two parts, mutually interactive: a vehicle model for the dynamic analysis and a model for the wear estimation. The entire model has been validated in collaboration with Trenitalia S.P.A, which has provided the technical documentation and the experimental results relating to some tests performed with the vehicle ALn 501 "Minuetto" on the Aosta-Pre Saint Didier line.

1 INTRODUCTION

The wear at the wheel-rail interface is an important problem in railway field. The evolution of the profile shape due to wear has a deep effect on the vehicle dynamics and on its running stability, leading to performance variations both in negotiating curves and in straight track. Therefore the original profiles have to be periodically re-established by means of turning. In the development of an accurate wear model [1, 2, 3], one of the most critical aspect is the availability of experimental results, since the collection of the data requires at least a few months with relevant economic costs.

In this work authors will present a complete model to predict the evolution of wheel profiles due to wear that involves multibody simulations and a wear model. More precisely, the general layout adopted is made up of two parts mutually interactive: the vehicle model (multibody model and wheel-rail global contact model) and a wear model (local contact model, wear evaluation using the Reye hypothesis and wheel profile update). The multibody model is implemented with the commercial multibody code SIMPACK: the accurate three-dimensional dynamic modeling of the vehicle's motion takes into account all the significant degrees of freedom. The wear model evaluates in MATLAB the amount of removed material and its distribution along the wheel profile; the removal of material and the profile update are carried out considering the fully 3D structure of the phenomenon. The entire model has been validated thanks to the technical and experimental data related to the Aln 501 "Minuetto" vehicle and the measured wear progress provided by Trenitalia S.p.A. as well as the track data given by Rete Ferroviaria Italiana and relative to the statistical analysis of Aosta-Pre Saint Didier railway line.

2 GENERAL ARCHITECTURE OF THE MODEL

The general layout of the model has been arranged in agreement with Trenitalia S.p.A and RFI, according to the following main working hypotheses:

- discrete approach to the wear evolution, dividing the entire distance to be simulated in steps and updating the wheel profile after each step. The wheel profile used in the dynamic simula-

tions is the same for each vehicle's wheel and the output of the wear model is the evolution of a single mean wheel profile;

- the track is not subjected to wear and the rail profile are always new and kept constant;
- the abrasion is the unique considered wear mechanism and the wheel-rail contact is hypothesized under dry conditions.

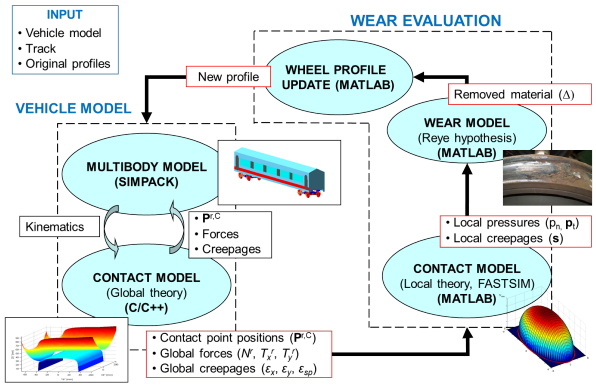

Figure 1: General architecture of the model.

The numerical evolution of the wheels shape is treated with a discrete approach. The entire mileage to be simulated is divided in a few spatial steps, in which the wheel profile is maintained constant during the simulations; the results of the wear evaluation, at the end of the current step, allow to update the wheel profile for the next step of the procedure. The step length depends on the total distance to be covered and it is one of most important aspect of the entire numerical procedure, because it directly affects the precision: in fact, the smaller is the step, the higher the accuracy and the overall computation time are; hence the choice has to be a compromise between these aspects.

A diagram representation of the whole model is visible in Fig. 1: it includes two main parts that work alternatively during each step. On the left there is the *vehicle model*, the part which is responsible for the dynamic simulations, made up of the multibody model and the global contact model developed by authors in previous work [4, 5]; the two subsystems interact online to each other during the simulations to reproduce the vehicle dynamics. On the right there is the *wear evaluation*, which comprises three sub-parts: the local contact model, the wear model and the wheel profile update. In more detail, during the dynamical simulations in the first task of each procedure step, the multibody model implemented in SIMPACK exchanges data continuously at each time step with the global contact model, passing the wheelset kinematic variables (wheelset position and orientation and their derivatives) and receiving the global contact variables (positions of the contact points $\mathbf{P}_c^r$, the wheel-rail contact forces N, T_x, T_y and the global creepages ϵ_x, ϵ_y, ϵ_{sp}). Once the multibody simulations are completed, the local contact model, (written in MATLAB and based on the FASTSIM algorithm [6]) evaluates, starting from the global contact variables, the contact pressures, the local creepages and consequently the total frictional work ($\mathbf{p}_t$, p_n, $\mathbf{s}$, L_F) inside each detected contact patch; the removed material and its distribution along the wheel profile are then obtained passing these data to the wear model, by means of the Reye hypothesis [1, 2, 3]. Finally, the wheel profile is updated through suitable numerical procedures.

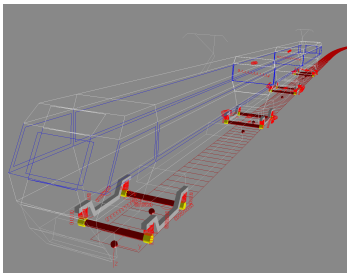

Figure 2: The Aln 501 Minuetto multibody model.

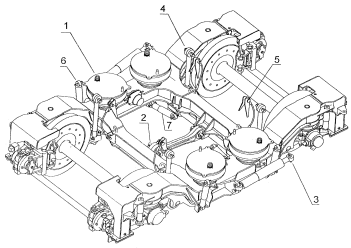

Figure 3: The Jacobs bogie.

3 THE VEHICLE MODEL

3.1 *The Multibody Model*

The railway vehicle on which this study has been performed is the ALn 501 Minuetto (Fig. 2). It is made up of three coaches and four bogies with two wheelsets; the external bogies are motorized whereas the two intermediate trailer bogies are of Jacobs type, shared between two coaches (Fig. 3).

As in the most part of passenger trains, the bogies are provided with two stages of suspensions. The primary suspensions, which link the axleboxes with the bogie frame, are constituted by Flexicoil springs, made up of two coaxial springs, which mainly provide the vertical stiffness in this stage. A non linear damper is responsible for the damping of the vertical relative displacements. The secondary suspension stage comprises two airsprings (four in the Jacobs bogie) for the vertical, longitudinal and lateral stiffness (used to guarantee passengers comfort and a simple automatic regulation of the coaches height with changes in the vertical loads), a non linear longitudinal rod (to transmit the traction and braking efforts), a torsion bar (to provide the correct rolling stiffness), non linear lateral bumpstops and non linear dampers (lateral, vertical and anti-yaw). All the described devices have been modeled as viscoelastic force elements, taking into account all the mechanical non linearities [7, 8]. The resultant whole SIMPACK multibody model includes 31 rigid bodies: 3 coaches, 4 bogie frames, 8 wheelsets and 16 axleboxes.

3.2 *The Global Contact Model*

The global contact model allows to perform an online calculation of the contact forces at the wheel-rail interface during the multibody simulations. The model is based on a semianalytic approach that guarantees high numerical efficiency, the online implementability directly within the multibody models without look-up tables and in general numerical performance better than those obtainable with commercial softwares (Vi-Rail, SIMPACK) [4, 5].

The contact model consists of two sequential phases: the research of the contact points and the computation of the normal and tangential actions in each contact patch. The first task is entrusted to an algorithm developed by authors in previous works (the DIST method [4, 5]) that takes into account the original multi-dimensional contact problem and reduces it to a simpler scalar problem, which can be easily handled by means of numerical methods, with remarkable advantages in terms of management of both the multiple solutions and the computational load. The algorithm for the detection of contact points is based on the standard idea that the distance between the wheel surface and the rail surface is stationary in the considered points [9].

Two reference systems are introduced to formulate the problem: the *auxiliary system* $O_r x_r y_r z_r$ and the *local system* $O_w x_w y_w z_w$. The first system moves along the track centerline following the wheelset: the x_r is tangent to the centerline in the O_r point while the z_r axis is perpendicular to

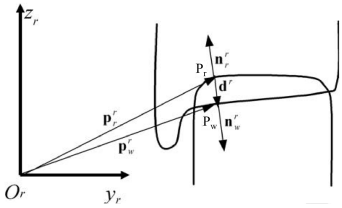

Figure 4: The distance method.

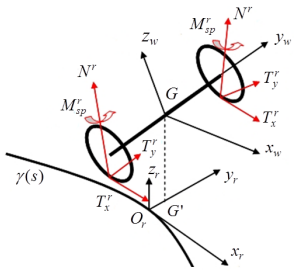

Figure 5: Nomenclature of the contact forces.

the plane of track; the position of O_r can be determined imposing that the $y_r z_r$ plane contains the wheelset centre of mass G_w. The local system is fixed on the wheelset, except for the rotation around the wheelset axle: in particular, $O_w \equiv G_w$ and y_w coincides with the wheelset rotation axis. In the following $\mathbf{p}_w^r$ and $\mathbf{p}_w^w$ will be the positions of a point on the wheel in the auxiliary system and in the local system respectively, while the position of a point on the rail surface in the auxiliary system will be indicated with $\mathbf{p}_r^r$. At this point, the geometrical conditions can be stated as follows (Fig. 4):

- the normal unitary vector relative to the rail surface $\mathbf{n}_r^r(\mathbf{p}_r^r)$ and the wheel surface unitary vector $\mathbf{n}_w^r(\mathbf{p}_w^r)$ have to be parallel ($\mathbf{R}_2$ is the rotation matrix that links the local system to the auxiliary one):
$$\mathbf{n}_r^r(\mathbf{p}_r^r) \times \mathbf{n}_w^r(\mathbf{p}_w^r) = \mathbf{n}_r^r(\mathbf{p}_r^r) \times \mathbf{R}_2 \mathbf{n}_w^w(\mathbf{p}_w^w) = \mathbf{0}; \tag{1}$$
the wheel and rail surfaces can be locally considered as a revolution and an extrusion surface respectively: $\mathbf{p}_w^{w\,T} = (x_w, y_w, -\sqrt{w(y_w)^2 - x_w^2})$, $\mathbf{p}_r^{r\,T} = (x_r, y_r, r(y_r))$, where the generative function $w(y_w)$ and $r(y_r)$ are supposed to be known;

- the rail surface normal unitary vector $\mathbf{n}_r^r(\mathbf{p}_r^r)$ and the distance vector $\mathbf{d}^r = \mathbf{p}_w^r - \mathbf{p}_r^r$ between the generic point of the wheel and of the rail have to be parallel:
$$\mathbf{n}_r^r(\mathbf{p}_r^r) \times \mathbf{d}^r = \mathbf{0}. \tag{2}$$

The distance between the generic points on the wheel and on the rail can be expressed as

$$\mathbf{d}^r(x_w, y_w, x_r, y_r) = \mathbf{p}_w^r(x_w, y_w) - \mathbf{p}_r^r(x_r, y_r) = \mathbf{o}_w^r + \mathbf{R}_2 \mathbf{p}_w^w(x_w, y_w) - \mathbf{p}_r^r(x_r, y_r); \tag{3}$$

thus, it depends on the four parameters (x_w, y_w, x_r, y_r), that identify a point on both the surfaces. The Eq. 1 and 2 constitute a system of six scalar equations and four unknowns (x_w, y_w, x_r, y_r) (only four of the equations are independent). As previously stated, the problem can be reduced to a scalar equation in the unknown y_w expressing x_w, x_r, and y_r as functions of y_w. By means of suitable analytical procedures, from the second component of (1) the expression $x_{w1,2}(y_w)$ (two possible values are present) can be obtained; then, similarly, from the first component of (1) the expression for $y_{r1,2}(y_w)$ can be determined and from the second component of (2) the relation $x_{r1,2}(y_w)$ can be obtained. Finally, replacing the variables $x_{w1,2}(y_w)$, $x_{r1,2}(y_w)$ and $y_{r1,2}(y_w)$ in the first component of (2), two simple scalar equations in the y_w variable has been found, easy to solve numerically with the advantages previously mentioned (in the following y_{w1j}^C and y_{w2k}^C with $1 \leq j \leq n_1$ and $1 \leq k \leq n_2$, will be the generic solution of these equations). For each y_w^C, the values of the unknowns x_w^C, x_r^C, y_r^C and consequently the contact point positions on the wheel and the rail $\mathbf{p}_w^{r,C} = p_w^r(x_w^C, y_w^C)$ and $\mathbf{p}_r^{r,C} = p_r^r(x_r^C, y_r^C)$ can be determined by substitution. Once

$x_w^C, y_w^C, x_r^C, y_r^C$ are determined, the physical conditions of no penetration between wheel and rail and the convexity condition have to be satisfied so that the contact is physically possible.

For each contact point the global creepages acting in the contact patch and the normal and tangential contact forces, evaluated by means of the Hertz's and the Kalkers global theory respectively, are determined (Fig. 5)[6].

4 THE WEAR EVALUATION

4.1 *The Local Contact Model*

The local contact model starts from the global contact variables evaluated by the vehicle model (contact points position, contact forces and spin moments, global creepages and patch semiaxes) and calculates the local contact variables (normal pressures, tangential stresses and creepages) within each contact patch. The model is based on an approximate but very efficient version of the Kalker's local theory implemented in his FASTSIM algorithm [6], commonly used in railway multibody simulations. The algorithm works in a local reference system, whose origin is situated in the centre of the elliptical contact patch, with the x,y axis defined in the common tangent plane to the contact surfaces (Fig. 6).

The working hypothesis on which the algorithm is developed is the proportionality between the tangential pressure $\mathbf{p}_t$ and the elastic displacements $\mathbf{u}$ in a generic point of the contact patch:

$$\mathbf{u}(x,y) = L\mathbf{p}_t(x,y); \qquad L = L(\boldsymbol{\epsilon}, a, b, G, \nu) \tag{4}$$

where the flexibility L is a function of the global creepage vector $\boldsymbol{\epsilon}$, the ellipse semiaxes a, b, the combined shear modulus G and the combined Poisson's coefficient ν [6].

The calculation of the local variables p_n, $\mathbf{p}_t$ and $\mathbf{s}$ is performed in each point of the grid adopted to mesh the contact patch (Fig. 6): the longitudinal grid resolution is not constant and increases in the nearby of the lateral edges of the ellipse, where the length $a(y)$ are shorter. So, the accuracy near the edge is appreciably higher than that obtainable with a constant resolution grid, that would produce more numerical errors.

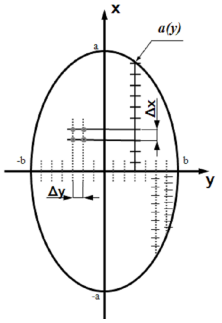

Figure 6: Contact patch discretization.

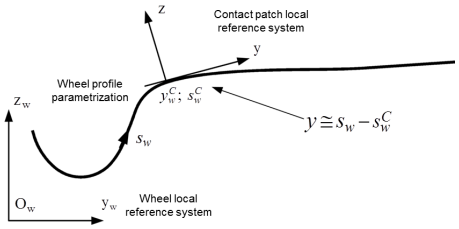

Figure 7: Wheel profile parametrization.

4.2 *The Wear Model*

The calculation of the abrasive wear on the wheel is based on a three-dimensional variant of the Reye hypothesis which states the proportionality between the volume of removed material and the total frictional work: $\delta V = C\delta L_F$. The main output of the wear model is $\delta_{P_{wi}^{jk}(t)}(x,y)$, expressed

in mm^3/(mm^{2}m), a function of the time which describes the specific volume (the volume per unit of area and per unit of traveled distance) of removed material due to the wear in the i-th contact patch of the j-th wheel in the k-th multibody simulation of the statistical analysis of the track. The three indexes just introduced are variable in the following intervals: $1 \leq j \leq N_W$ where N_W is the number of the vehicle's wheels, $1 \leq i \leq N_P$ where N_P is the maximum allowed number of the contact points (as will be explained below) and $1 \leq k \leq N_C$ with N_C equal to the number of the multibody simulations in the statistical description of the real track.

The quantity $\delta_{P_{wi}^{jk}(t)}(x, y)$ has to be evaluated in each point (x_h, y_l) of the contact patch grid. To this aim, the local frictional power in these points can be estimated by means of the *wear index* $I_W = (\mathbf{p_t} \cdot \mathbf{s})/V$ (N/mm^2), which is experimentally related to the *wear rate* K (μg/m·mm^2): the wear rate gives a measure of the amount of material removed per meter of traveled distance by the train and per mm^2 of surface. The analytic expression for $K(I_W)$ is given by Eq. 5 [1, 3].

$$K_W(I_W) = \begin{cases} 5.3 \cdot I_W & I_W < 10.4 \quad \text{N/mm}^2 \\ 55.0 & 10.4 \leq I_W \leq 77.2 \quad \text{N/mm}^2 \\ 61.9 \cdot I_W & I_W > 77.2 \quad \text{N/mm}^2 \end{cases} \tag{5}$$

After the evaluation of the wear rate, the specific volume $\delta_{P_{wi}^{jk}(t)}(x, y)$ can be calculated as follows:

$$\delta_{P_{wi}^{jk}(t)}(x, y) = \frac{K(I_W)}{\rho} \qquad \left(\frac{\text{mm}^3}{\text{m mm}^2}\right) \tag{6}$$

in which ρ is the material density (expressed in kg/m^3).

4.3 *The Profile Update*

The profile update is the part of the whole architecture which provides, by means of numerical procedures, the wheel profile for the next step $r_n(y_w)$ starting from the profile used at the current step $r_p(y_w)$ and exploiting the results of the wear model. It is surely a key point of the procedure since the adopted strategy may appreciably affects the results. The importance of this task is due to a series of distinct issues: in particular the necessity to generate as output of the wear model a single wheel profile and the need to avoid numerical noise on the distribuition $\delta_{P_{wi}^{jk}(t)}(x, y)$.
The numerical procedures which provide the new profile are described below:

1) Longitudinal integration:

$$\frac{1}{2\pi w(y_{wi}^{jk})} \int_{-a(y)}^{a(y)} \delta_{P_{wi}^{jk}}(x, y)dx = \delta_{P_{wi}^{jk}(t)}^{tot}(y) \qquad \left(\frac{\text{mm}^3}{\text{m mm}^2}\right); \tag{7}$$

this operation sums all the wear contributions in the longitudinal direction and spreads them along the circumference of the wheel.

2) Time integration:

$$\int_{T_i}^{T_f} \delta_{P_{wi}^{jk}(t)}^{tot}(s_w - s_{wi}^{jk,C}(t))V(t)dt \cong \Delta_{P_{wi}^{jk}}(s_w) \qquad \text{(mm)}; \tag{8}$$

where $y \cong s_w - s_{wi}^{jk,C}$ (Fig. 7); s_w is the generic curvilinear abscissa of the wheel profile, $s_{wi}^{jk,C}(t)$ is the curvilinear abscissa of the contact point on the wheel at the time t and $V(t)$ is the vehicle speed. The integration performs the sum of all the contributions during the dynamic simulation: the result is the depth of material to be removed due to the considered contact point.

3) Sum on the contact points and average on the wheels and on the simulations:

$$\sum_{k=1}^{N_C} p_k \frac{1}{N_W} \sum_{j=1}^{N_W} \sum_{i=1}^{N_P} \Delta_{P_{wi}^{jk}}(s_w) = \bar{\Delta}(s_w); \tag{9}$$

this operation involves the sum on the N_P contact points for each wheel, the average on the N_W wheels and the weighted average on the N_C simulations. As explained in next paragraph, the p_k, $1 \leq k \leq N_C, \sum_{i=1}^{N_C} p_k = 1$ are the normalized weights related to the tracks of the statistical analysis. The contact patches are usually less than N_P and their number can vary during the simulation; hence, since the sum is extended to N_P, the contribution of the missing points has been automatically set equal to zero.

4) Scaling of the mileage:

Since an appreciable evolution of the wheel profile requires thousands of kilometers to manifest itself, the scaling of the distance becomes critically important to get results in a reasonable time. Although the real chosen mileage km_{tot} that the vehicle has to run is divided in discrete steps of length km_{step}, the step length is still excessive for the multibody approach and thus the scaling of Eq. 10 is adopted:

$$\bar{\Delta}(s_w)\frac{km_{step}}{km_{runs}} = \bar{\Delta}^{sc}(s_w). \tag{10}$$

The amount of removed material $\bar{\Delta}(s_w)$ depends on the overall mileage traveled by the vehicle during the N_C simulations, that is $km_{runs} = L_C$, where L_C is the length of curved tracks on which the results of the vehicle dynamics are evaluated. After the scaling, the quantity $\bar{\Delta}^{sc}(s_w)$ is related to a spatial step with a length equal to km_{step}, instead of km_{runs}. The chance to take advantage of the scaling lies in the linearity of the wear model with respect to the traveled distance.

5) Smoothing of the amount of removed material:

$$\Im\left[\bar{\Delta}^{sc}(s_w)\right] = \bar{\Delta}^{sc}_{sm}(s_w). \tag{11}$$

This procedure aims to realize the tuning of the model (to include the effect of other wear mechanisms), the filtering of numerical noise and the removal of physically meaningless short spatial wavelengths on the wheel profile. The numerical noise and the short wavelength contributions are treated with a discrete filter: a moving mean with a window width equal to the $1\% \div 5\%$ of the total number of points that discretize the wheel profile.

6) Profile update:

$$\begin{pmatrix} y_w(s_w) \\ r_p(y_w(s_w)) \end{pmatrix} - \bar{\Delta}^{s}_{sm}(s_w)\mathbf{n}^r_r \xrightarrow{re-parametrization} \begin{pmatrix} y_w(s^*_w) \\ r_n(y_w(s^*_w)) \end{pmatrix} \tag{12}$$

Finally, the profile for the next step is obtained removing the material in the normal direction from the current profile $r_p(s_w)$ (according to the function $\bar{\Delta}^{s}_{sm}(s_w)$) and then performing a new parametrization, to get again a curve parametrized by means of the curvilinear abscissa.

5 STATISTICAL APPROACH TO THE TRACK - MODEL VALIDATION

5.1 *The Aosta-Pre Saint Didier line*

The statistical approach to the track has been chosen to reduce and rationalize the total simulation work, avoiding excessively long simulations on the real track (see Tab. 1). The idea is to substitute the simulation on the whole track with an equivalent set of simulations on short curved tracks. More precisely, a set of radius curve classes characterized by a minimum R_{min} and a maximum R_{max} were identified analyzing the database provided by RFI and each of these was furthermore divided in superelevation subclasses. For each subclass a representative radius R_m was calculated by means of a weighted average on all the curve radii included in that subclass (using the length of curve as weighting factor) and the correspondent representative superelevation h was chosen as the

most frequent superelevation among the values found in that subclass. For each subclass a speed value V was chosen as the minimum value between the max speed allowable on the track (equal to $V_{max} = 70\,\text{km/h}$) and the speed calculated imposing a non-compensated acceleration of $0.6\,\text{m/s}^2$. Finally, a weighting factor p_k was introduced for each subclass to consider their frequency in the track and to diversify the wear contributions of the different subclasses.

R_{min} (m)	R_{max} (m)	Superelevation class $h_{min} - h_{max}$ (mm)	R_m (m)	h (mm)	V (km/h)	p_k %
147.1	156.3	0	-	-	-	-
		10 - 40	-	-	-	-
		60 - 80	-	-	-	-
		90 - 120	150	120	55	0.77
		130 - 160	-	-	-	-
156.3	166.7	0	-	-	-	-
		10 - 40	-	-	-	-
		60 - 80	-	-	-	-
		90 - 120	160	110	55	0.48
		130 - 160	165	140	55	0.56
166.7	178.6	0	-	-	-	-
		10 - 40	-	-	-	-
		60 - 80	-	-	-	-
		90 - 120	170	110	55	0.82
		130 - 160	175	130	55	1.55
178.6	192.3	0	-	-	-	-
		10 - 40	-	-	-	-
		60 - 80	-	-	-	-
		90 - 120	190	100	55	8.37
		130 - 160	180	130	55	0.45
192.3	208.3	0	-	-	-	-
		10 - 40	-	-	-	-
		60 - 80	-	-	-	-
		90 - 120	200	90	55	20.64
		130 - 160	200	130	60	4.00
208.3	227.3	0	-	-	-	-
		10 - 40	-	-	-	-
		60 - 80	220	80	55	0.70
		90 - 120	220	100	55	3.76
		130 - 160	-	-	-	-
227.3	250.0	0	-	-	-	-
		10 - 40	-	-	-	-
		60 - 80	240	80	55	7.26
		90 - 120	240	110	60	5.28
		130 - 160	-	-	-	-
250.0	312.5	0	-	-	-	-
		10 - 40	-	-	-	-
		60 - 80	270	70	55	3.91
		90 - 120	270	90	60	5.29
		130 - 160	-	-	-	-
312.5	416.7	0	-	-	-	-
		10 - 40	-	-	-	-
		60 - 80	370	60	55	2.26
		90 - 120	345	100	70	1.63
		130 - 160	-	-	-	-
416.7	∞	0	∞	0	70	32.27

Table 1: The N_C tracks of the statistical approach.

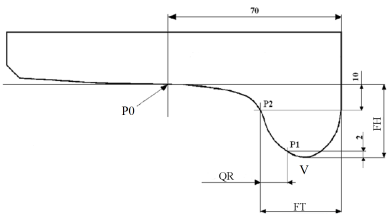

Figure 8: Reference dimensions.

Vehicle	km	QR	FH	FT
MD061	0	10.8	28.0	32.5
	1426	9.8	28.2	31.5
	2001	9.1	28.1	30.8
	2575	8.6	28.0	30.2
MD068	0	10.8	28.0	32.5
	1050	10.0	28.0	31.8
	2253	8.5	28.0	30.2
	2576	8.4	28.0	32.5
MD082	0	10.8	28.0	32.5
	852	10.6	28.0	32.3
	1800	9.6	28.0	31.3
	2802	8.7	28.8	30.3
	3537	8.3	27.6	30.0

Table 2: Experimental data processed.

5.2 *Wheel Profile Reference Dimensions*

According to [10], the wear progress in a wheel profile can be easily represented through three reference dimensions, avoiding a complete detection of the shape: the *flange thickness* FT, the *flange height* FH and the QR dimension (Fig. 8). Because of the way the quotas are defined, they are positive and do not depend on the wheel rolling radius. The values of these parameters are measured periodically and allow to decide whether the profile has to be re-turned or not (if it is still possible), considering the maximum or minimum values suggested by the regulation in forces [10]. The check of the reference quotas aims to guarantee mainly the safety against the hunting and the derailment, as well as an acceptable running behavior. In regard to their physical meaning, both the flange thickness FT and the flange height FH describe the size of the flange, while the flange height is also a measure of the wear on the wheel tread. The QR dimension gives information about the flange conicity.

5.3 *Treatment of the Experimental Data*

The experimental data provided by Trenitalia and RFI are related only to the wheel wear and consists in the wear control parameters measured as a function of the total distance traveled by the considered vehicle *Aln 501 Minuetto*. Particularly, the data have been measured on three different vehicles operating on the same track that are conventionally called MD061, MD068, MD082 and the reference quotas values have been measured for all the vehicle wheels. The data have been pre-processed by evaluating the arithmetic mean on all the sixteen vehicle wheels in order to obtain a single wheel profile that can be effectively compared with the simulated profile and to reduce the measurement errors (see Tab. 2).

5.4 *Progress of the Reference Dimensions and of the Wheel Profile*

This section presents the first results of the validation, showing the comparison between the numerically evaluated progresses of the three dimensions (FT, FH and QR) and the experimental data. The optimal filter parameters (especially the width of the window) have been picked out to minimize the global error.

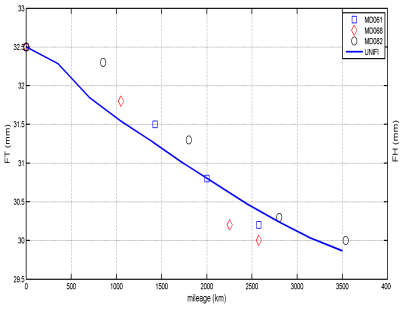

Figure 9: FT progress.

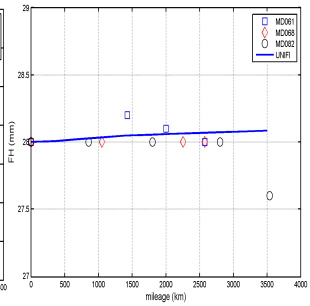

Figure 10: FH progress.

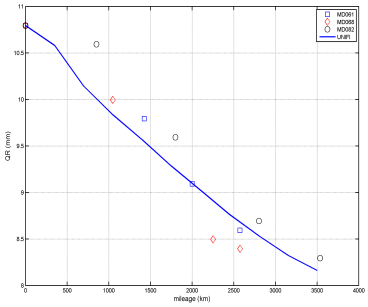

Figure 11: QR progress.

The progress of the FT dimension is shown in Fig. 9; the decrease of the quota is almost linear with the traveled mileage except in the first phases, where the profiles of wheel and rail are not conformal enough. The FH curve progress is presented instead in Fig. 10, which shows that, due to the presence of many sharp curves in the track and to the low traveled mileage, the wear is localized mainly on the flange rather than on the tread; thus the flange height remains nearly constant. The comparison between the real and simulated QR is finally shown in Fig. 11: the dimension decreases almost linearly too, leading to an augmentation of the conicity on the flange. As a conclusion, the comparisons show that the results of the wear model are quite consistent with the experimental data, both for the flange dimensions (FT, FH) and the QR; therefore the validation of the model can be considered satisfactory.

The numerical evolution of the wheel profile is presented in Fig. 12. Due to the low covered mileage and to the sharpness of the track, the wear is mainly localized on the flange rather than on the tread, where it is quite low and involves a slight reduction of the rolling radius.
Observing the flange zone, the wear rate is higher during the first steps because of the non-conformal contact due to the coupling between the ORE S1002 wheel profile and the UIC60 rail with an inclination of 1:20 rad; then it decreases becoming more regular and constant in the last phases, when the contact is more and more conformal (Fig. 13).

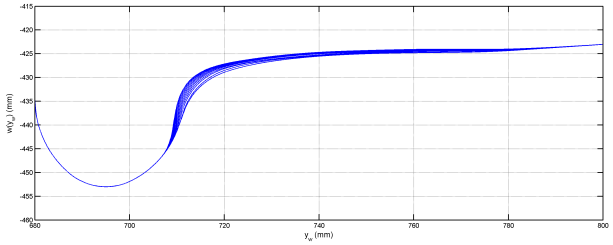

Figure 12: Evolution of the wheel profile.

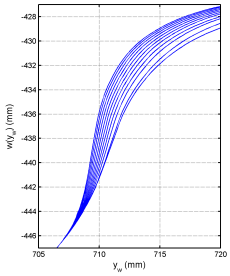

Figure 13: Evolution in the flange zone.

6 CONCLUSIONS

In this work the Authors have presented a complete model for the wheel wear prediction in railway applications. The entire model has been validated by exploiting the experimental data relative to a particularly critical scenery in terms of wear in the Italian railways: the ALSTOM Aln 501 "Minuetto" circulating on the Aosta–Pre Saint Didier railway line. A statistical approach to describe the track has been used to reduce the total computational effort. The arising model reproduces properly the evolution of all the three characteristic dimensions of the wheel profile which describe the wear progress. The resultant wheel profile evolution highlights that, in this particular application, the wear is severe and strongly localized on the flange of wheel because of both the sharpness of the track and the low covered mileage considered, leading to frequent maintenance interventions. Future developments may consist in the evaluation of the rail wear evolution and the implementation of other wear mechanisms such as fatigue wear and plastic wear.

7 ACKNOWLEDGEMENTS

Authors would like to thank Engg. R. Cheli and G. Grande of Trenitalia S.p.A for providing and giving the permission to edit the data relative both to the vehicle ALn 501 Minuetto and to the wheel wear evolution; a special thanks also goes to the Engg. R. Mele and M. Finocchi of Rete Ferroviaria Italiana for the data relative to the Aosta-Pre Saint Didier line.

References

[1] F. Braghin, R. Lewis, R. Dwyer-Joyce, S. Bruni, A mathematical model to predict railway wheel profile evolution due to wear, Wear 261 (2006) 1253–1264.

[2] T. Telliskivi, U. Olofsson, Wheel-rail wear simulation, Wear 257 (2004) 1145–1153.

[3] R. Enblom, M. Berg, Simulation of railway wheel profile development due to wear: influence of disk braking and contact environment, Wear 258 (2005) 1055–1063.

[4] E. Meli, S. Falomi, M. Malvezzi, A. Rindi, Determination of wheel-rail contact points with semianalytic methods, Multibody System Dynamics 20 (4) (2008) 327–358.

[5] M. Malvezzi, E. Meli, J. Auciello, S. Falomi, Dynamic simulation of railway vehicles: wheel - rail contact analysis, Vehicle System Dynamics 47 (7) (2009) 867–899.

[6] J. J. Kalker, Three-dimensional Elastic Bodies in Rolling Contact, Kluwer Academic Publishers, Dordrecht, Netherlands, 1990.

[7] R. V. Dukkipati, J. R. Amyot, Computer Aided Simulation in Railway Dynamics, Dekker, New York, 1988.

[8] S. Iwinicki, The Manchester Benchmarks for Rail Vehicle Simulators, Swets & Zeitlinger, Lisse, Netherlands, 1999.

[9] F. Cheli, E. Pennestrì, Cinematica e dinamica dei sistemi multibody, CEA, 2006.

[10] EN 15313 - *Railway applications - In service wheelset operation requirements - In service and off-vehicle wheelset maintenance*.